

## ARTICLE OPEN



# Changes in land-atmosphere coupling increase compound drought and heatwaves over northern East Asia

Ye-Won Seo<sup>1,2</sup> and Kyung-Ja Ha<sup>1,3</sup>✉

Compound drought and heatwaves (DHW) events have much attention due to their notable impacts on socio-ecological systems. However, studies on the mechanisms of DHW related to land-atmosphere interaction are not still fully understood in regional aspects. Here, we investigate drastic increases in DHW from 1980 to 2019 over northern East Asia, one of the strong land-atmosphere interaction regions. Heatwaves occurring in severely dry conditions have increased after the late 1990s, suggesting that the heatwaves in northern East Asia are highly likely to be compound heatwaves closely related to drought. Moreover, the soil moisture–temperature coupling strength increased in regions with strong increases in DHW through phase transitions of both temperature and heat anomalies that determine the coupling strength. As the soil moisture decreases, the probability density of low evapotranspiration increases through evaporative heat absorption. This leads to increase evaporative stress and eventually amplify DHW since the late 1990s. In particular, seasonal changes in soil moisture and evapotranspiration between spring and summer contributed to the amplification of DHW by enhancing land-atmosphere interaction.

*npj Climate and Atmospheric Science* (2022)5:100; <https://doi.org/10.1038/s41612-022-00325-8>

## INTRODUCTION

Compound extreme events have been steadily increasing over recent decades, leading to significant environmental and social impacts<sup>1–5</sup>. For instance, the 2012 drought in the central U.S., accompanied by high-temperature anomalies, cost at least \$30 billion in large agricultural damage<sup>6</sup>. The heatwaves have been delivering havoc across Europe in 2022, causing droughts, wildfires, and deaths. These compound extreme events could contribute to the onset of wildfires as well as the onset of rapidly developing droughts, and their frequency is expected to increase<sup>7</sup>. Moreover, compound temperature and precipitation extreme events have decisive effects on the probability of increased crop losses<sup>8</sup>. Extreme temperature and precipitation events such as heatwaves and droughts have been widely investigated worldwide<sup>9–11</sup>. Therefore, understanding and investigating compound heat and precipitation extreme events is critical to mitigating significant social and economic risks.

Regional differences in temperature and hydrological variables, including precipitation, result in disparate spatial patterns for compound extreme heat events<sup>12,13</sup>. Compound droughts and heatwaves (DHW) develop according to the modulation of the variety of land surface fluxes affected by surface dryness, climate patterns, and anthropogenic forcing<sup>14,15</sup>. Relevant large-scale effects of external forcing on extreme heat events include net increases in temperature induced by changes in the enhanced moisture content of the atmosphere, radiation, and circulation patterns. Additional feedback processes related to land-atmosphere interactions associated with soil moisture or snow can modulate global changes in extreme heat events<sup>10,16–20</sup>. Previous studies have shown that dry soil moisture conditions can significantly affect the severity of heatwaves and droughts by coupling the soil moisture and the atmosphere<sup>19,21</sup>. Soil moisture–temperature coupling could account for heatwaves in summer climates. Modeling experiments have focused on identifying strong coupling regions and determining how climate

change affects these regions<sup>16,22</sup>. Changes in the balance of soil moisture are increasingly being discussed in the recent climate change studies because of the important role of soil moisture in the land–atmosphere system.

Numerous studies have focused on the role of the interaction between land and atmosphere to examine the simultaneous occurrence of heatwaves and droughts<sup>17,21,23</sup>. Land surface states can contribute to extreme temperature events such as heatwaves, in particular, the number of heatwave days, through the surface energy balance coincident with soil moisture deficits<sup>16,24,25</sup>. For instance, Li et al.<sup>26</sup> highlighted the role of soil moisture–atmospheric feedback in future climate change, leading to increased temperature amplitude and interannual variability. In addition, previous studies using simulations of the Global Land-Atmosphere Coupling Experiment-Coupled Model Intercomparison Project Phase 5 revealed that drying trends in soil moisture tend to intensify high-temperature extremes and dryness<sup>27,28</sup>.

Soil moisture is a major variable of the land climate system because it can alter the transmission and distribution of water and energy on the land surface by changing the surface evapotranspiration, albedo, and soil thermal capacity. Previous studies have shown that land-atmospheric feedback processes induced by soil moisture anomalies participate in intensively controlling near-surface heat and dryness via high-pressure structures in the mid-troposphere<sup>19,20,25</sup>. Soil moisture continues to decrease in dry regions, and the temperature increases sharply, with a strong negative correlation. According to previous studies, arid and semi-arid regions will be more severely stressed by climate change<sup>12</sup>. Moreover, soil moisture/temperature interactions enhance temperature variability in summer, causing extreme temperature events as the soil moisture is dry<sup>16–20</sup>. Some studies have shown that dry soil with continuous anticyclonic circulation enhances soil moisture–temperature feedback, thereby increasing the surface temperature<sup>29–31</sup>. Recently, Zhang et al.<sup>10</sup> showed that the sudden increase in dry and hot extremes over inner East Asia has been

<sup>1</sup>Center for Climate Physics, Institute for Basic Science, Busan, South Korea. <sup>2</sup>Pusan National University, Busan, South Korea. <sup>3</sup>BK21 School of Earth and Environmental Systems, Pusan National University, Busan, South Korea. ✉email: [kjha@pusan.ac.kr](mailto:kjha@pusan.ac.kr)

associated with persistent soil moisture deficiency over the last two decades.

Increased land–atmosphere coupling is associated with persistent soil moisture deprivation, which exacerbates surface warming and anticyclonic circulation anomalies. Moreover, it strengthens the heatwaves that affect soil deficiency. Thus, land–atmosphere interactions could lead to large-scale heatwave events, suggesting that extreme temperature events intensify. Therefore, a better understanding of the relationship between soil moisture and temperature can help reduce the uncertainty in extreme heat projections. However, these studies have primarily been limited to Europe, with a gradually expanding scope of regional research. In particular, there are relatively few studies on the relationship between the soil moisture and temperature over East Asia, and how they affect changes in land–atmosphere interactions over East Asia has not been well discussed. At present, there are abrupt changes in compound extreme events related to severe heat during boreal summer over East Asia. This region was often severely affected by heatwaves and droughts and was been concentrated as a hotspot in DHW<sup>3,4</sup>. Some studies have attempted to suggest possible causes

from the connection with large-scale atmosphere circulation<sup>2</sup>. Some studies have explored the land–atmosphere interaction; however, their understanding has not been fully elucidated. Accordingly, this study aimed to identify the significant changes in compound heat events over East Asia using reanalysis datasets. In addition, this study explores the soil moisture–temperature coupling associated with heatwave events, and the relationship with evapotranspiration related to changes in soil moisture affecting compound heat events over East Asia.

## RESULTS

### Abrupt changes in compound droughts and heatwaves

Recent changes in land–atmosphere coupling can be quantified using soil moisture–temperature coupling diagnostics<sup>32</sup>. This metric quantifies the relationship between near-surface temperature anomalies and soil moisture deficiency in the surface energy balance. In the past two decades, the soil moisture–temperature coupling strength has strengthened significantly over East Asia (Fig. 1c, d). The most robust changes occurred where there was a

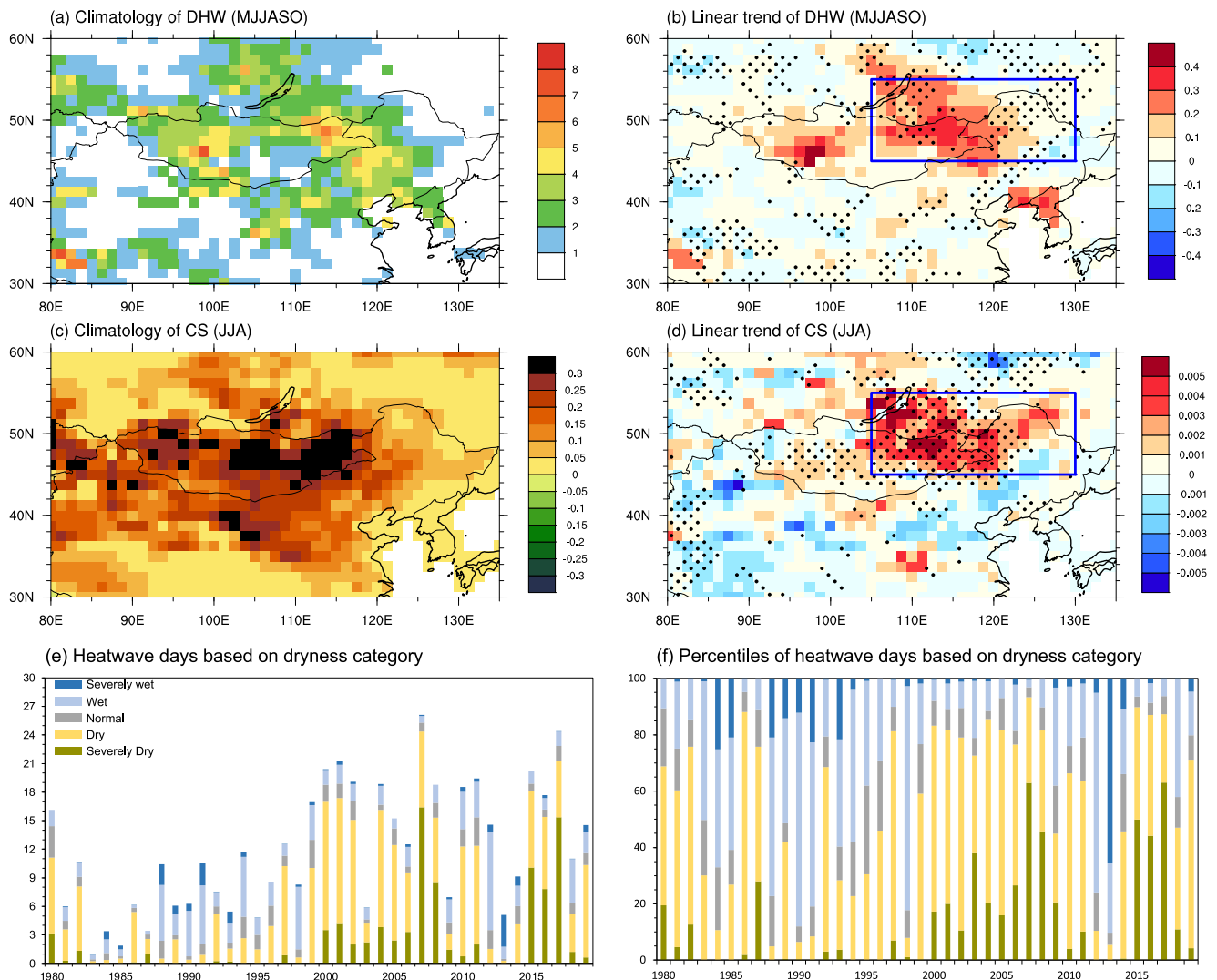


**Fig. 1** Linear trends of DHW and CS, and time series of DHW based on dryness category. Climatology of (a) dry heatwave (DHW) during warm season (MJJASO) (days year<sup>-1</sup>) and (c) soil moisture–temperature coupling strength index (CS) during summer (JJA) for the period 1980–2019 and (b), (d) their linear trends. The dots in (b) and (d) denote the 90% confidence level using the *P* value. Time series of (e) heatwave days based on dryness category and (f) its percentiles during the period 1980–2019 over East Asia [105–130°E, 45–55°N]. The dryness categories are distinguished based on scPDSI; severely dry (scPDSI < -3), dry (-3 < scPDSI < -0.5), normal (-0.5 < scPDSI < 0.5), wet (0.5 < scPDSI < 3), and severely wet (scPDSI > 3).

significant increase in DHW, including in northeastern Mongolia (Fig. 1a, b). Hereafter, we focus on the specific regions (blue box in Fig. 1b, d) where heatwaves and soil moisture–temperature coupling strengthened for the period from 1980 to 2019 (Fig. 1b, d) (See “Methods”). The total number of heatwave days under various dryness conditions (severely dry, dry, normal, wet, and severely wet) indicates that heatwaves occur more frequently in dry conditions than in wet conditions over northern East Asia (Fig. 1e, f). These characteristics reflect the geographic nature of the region near the Gobi Desert. Heatwaves under dry conditions occur frequently, and severely dry conditions have intensified since the late 1990s. Following the change point detection (See “Methods”), we investigated the differences in land–atmosphere interactions during two periods based on the detected change point, 1999 (Supplementary Fig. 1). Hereafter, the two periods are named the BEF1999 (1980–1998) and AFT1999 (1999–2019). The heatwaves in dry and severely dry conditions in the AFT1999 period have occurred about 1.2 and 5.3 times more than in the BEF1999 period, respectively (Fig. 1e). This implies that recent heatwaves in northern East Asia are more likely to take the form of the DHW, which is closely related to drought. We obtained results similar to Fig. 1 by conducting the same analysis using ERA-Interim datasets (Supplementary Fig. 2). These results are consistent with previous studies based on a tree-ring-based reconstruction of heatwaves<sup>10</sup>. They suggested that the intensified land–atmosphere interaction related to persistent soil moisture deficiency enhances surface warming and an anomalous high system, and it plays an important role in amplifying heatwaves that exacerbate soil drying.

### Changes in the relationship between evapotranspiration and soil moisture

To understand the detailed soil moisture–temperature coupling processes between the two periods, a composite analysis of temperature and energy anomalies was performed (Fig. 2). The figure shows the temperature anomaly ( $T'$ ) and the heat anomaly ( $H' - H'_p$ ), which determine the soil moisture–temperature coupling strength over two periods. Although the spatial distributions of the heat and temperature anomalies were somewhat different, their phases were identical during the two periods. Temperature and heat anomalies exhibited negative values during BEF1999 period but changed to positive values during AFT1999 period (Fig. 2c, d). The phase changes in temperature and heat anomalies affected the enhanced land–atmosphere interaction. In particular, the correlation coefficient between the heat anomaly and coupling strength changed from 0.12 in the BEF1999 period to 0.85 in the AFT1999 period (Fig. 2g). This result indicates that the evaporative stress of AFT1999 period increased because of the increased soil moisture deficiency<sup>32</sup>. The correlation between the temperature anomaly and coupling strength index changed from  $-0.32$  in the BEF1999 period to  $0.65$  in the AFT1999 period (Fig. 2g). The heat and temperature anomalies show opposite correlations during BEF1999 period and act in the direction of decreasing coupling strength; however, since the late 1990s, both anomalies have strengthened their connection with coupling strength. Therefore, the phase transitions of the heat and temperature anomalies amplified the DHW by increasing the soil moisture–temperature coupling strength.

According to Dirmeyer et al.<sup>33</sup>, the correlation between soil moisture and evapotranspiration can be used to represent the land–atmosphere coupling state. The energy supply induced by abnormal atmospheric conditions changes evapotranspiration, which reduces soil moisture. In dry regions, soil moisture can change evapotranspiration through evaporative heat absorption, and weakened evapotranspiration increases temperature<sup>34</sup>. To examine the relationship between soil moisture, evapotranspiration, and soil moisture–temperature coupling strength, their probability density functions in summer (JJA) during the two

periods were analyzed (Fig. 3). Under dry soil moisture conditions and low evapotranspiration, land–atmosphere coupling was insensitive to the amount of soil moisture during both periods (Fig. 3a, b, d, e). Moreover, the probability density was relatively high for wet soils, however, the coupling strength was rather low (Fig. 3b, e). During AFT1999 period, the coupling strength associated with soil moisture and evapotranspiration increased slightly, however, the shape of the probability density was not significantly changed (Fig. 3d, e). On the other hand, changes in the probability density of soil moisture and evapotranspiration were evident (Fig. 3f). Since the late 1990s, an evapotranspiration density of less than  $3 \text{ mm day}^{-1}$  has increased as soil moisture has decreased. This indicates that evapotranspiration in this region is strongly controlled by soil moisture. Thus, the region has changed from an energy-limited evapotranspiration regime to a soil moisture-limited regime<sup>35</sup>. This relationship is closely linked to the sensible heat flux, which induces an increase in surface temperature. In addition, the increased temperature leads to soil moisture deficiency and additional evapotranspiration demand, and it works as positive feedback in dry regions. This corresponds to the previous studies that suggested that the low soil moisture plays a role in intensifying heatwaves and affects the predictability of interannual variation in precipitation over Mongolia<sup>36,37</sup>.

Dry persistent soil conditions enhance surface sensible heat fluxes and limit evapotranspiration, leading to increased surface temperature<sup>38</sup>. Although many studies have reported heatwave amplification through a feedback loop between soil moisture deficiency and summer temperature<sup>28,39</sup>, the soil moisture–temperature couplings are strong in spring as well as in summer over northern East Asia<sup>40</sup> (Supplementary Fig. 3). Therefore, this study aimed to reveal how seasonal evapotranspiration and soil moisture changes from spring (MAM) to summer (JJA) influence heatwaves and changes in coupling strength. In other words, this study focused on the effect of the persistence of soil moisture deficiency from spring. During the BEF1999 period, the seasonal changes in soil moisture slightly influenced the occurrence of the heatwaves; however, the seasonal changes in evapotranspiration showed a negative relationship with heatwaves (Fig. 4a, c). The regression coefficients of heatwave frequency against seasonal changes in soil moisture and evapotranspiration show that these seasonal changes are highly related to the occurrence of heatwaves during AFT1999 period (Fig. 4b, d). To clarify the connection between soil moisture and evapotranspiration, a scatter plot of the seasonal differences between soil moisture and evapotranspiration is presented in Supplementary Fig. 4. Changes in soil moisture were positively correlated with evapotranspiration during AFT1999 period (Supplementary Fig. 4b). The correlation between seasonal changes in soil moisture and evapotranspiration was  $-0.30$  and  $0.52$  during the BEF1999 period and AFT1999 periods, respectively (Supplementary Fig. 4c). This can be explained by the impact of soil moisture on the land–atmosphere interaction limited evapotranspiration regimes, which are linked to a dry transitional soil moisture regime<sup>35,41</sup>. As the soil moisture decreased, the remaining moisture became less accessible for plant uptake (and bare soil evaporation). However, the proportion of available energy entering the latent heat flux (and thus evapotranspiration) decreases, increasing sensible heat<sup>16,35</sup> and consequently feedbacks on temperature<sup>42</sup>. Furthermore, significant linkages were identified in areas with predominantly low vegetation, which comprised 57.3% short grass and 35.4% crops, and mixed farming (Supplementary Fig. 5, Supplementary Table 1), where low vegetation covered more than 10% (Supplementary Fig. 4b). This implies that the change in the relationship between soil moisture and evapotranspiration during AFT1999 period was triggered by soil moisture deficiency. A composite analysis was performed to examine the land–atmosphere coupling strength according to the soil moisture amount during the summer (Supplementary Fig. 6). The coupling strength anomalies were higher in dry soil years than in wet soil years, and the differences were significantly dominant. Soil moisture deficiency

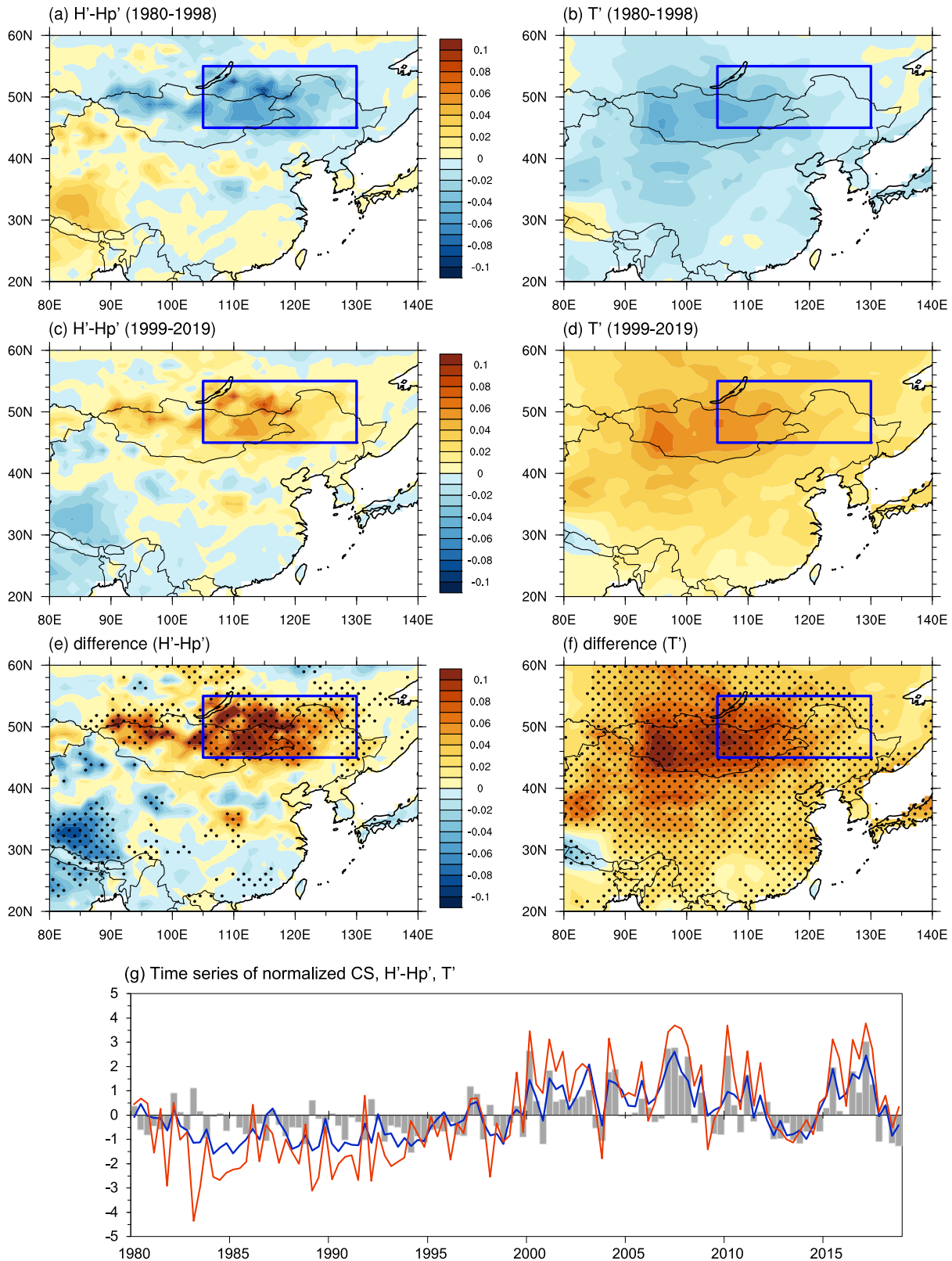


**Fig. 2 Composite of energy and temperature anomalies and its normalized monthly time series during summer.** Energy anomalies ( $H' - H_p'$ ) and temperature anomalies ( $T'$ ) during the period **(a, b)** 1980–1998, **(c, d)** 1999–2019, and **(e, f)** its differences over East Asia, respectively. The dots in **(e)** and **(f)** denote the 95% confidence level based on the Student's  $t$  test. **g** Monthly time series of normalized soil moisture-temperature coupling strength index (CS) (gray bars),  $H' - H_p'$  (orange line), and  $T'$  (blue line) in summer (June–July–August). The regions contributing to the time series are marked in blue boxes [105–130°E, 45–55°N] in **(a–f)**.

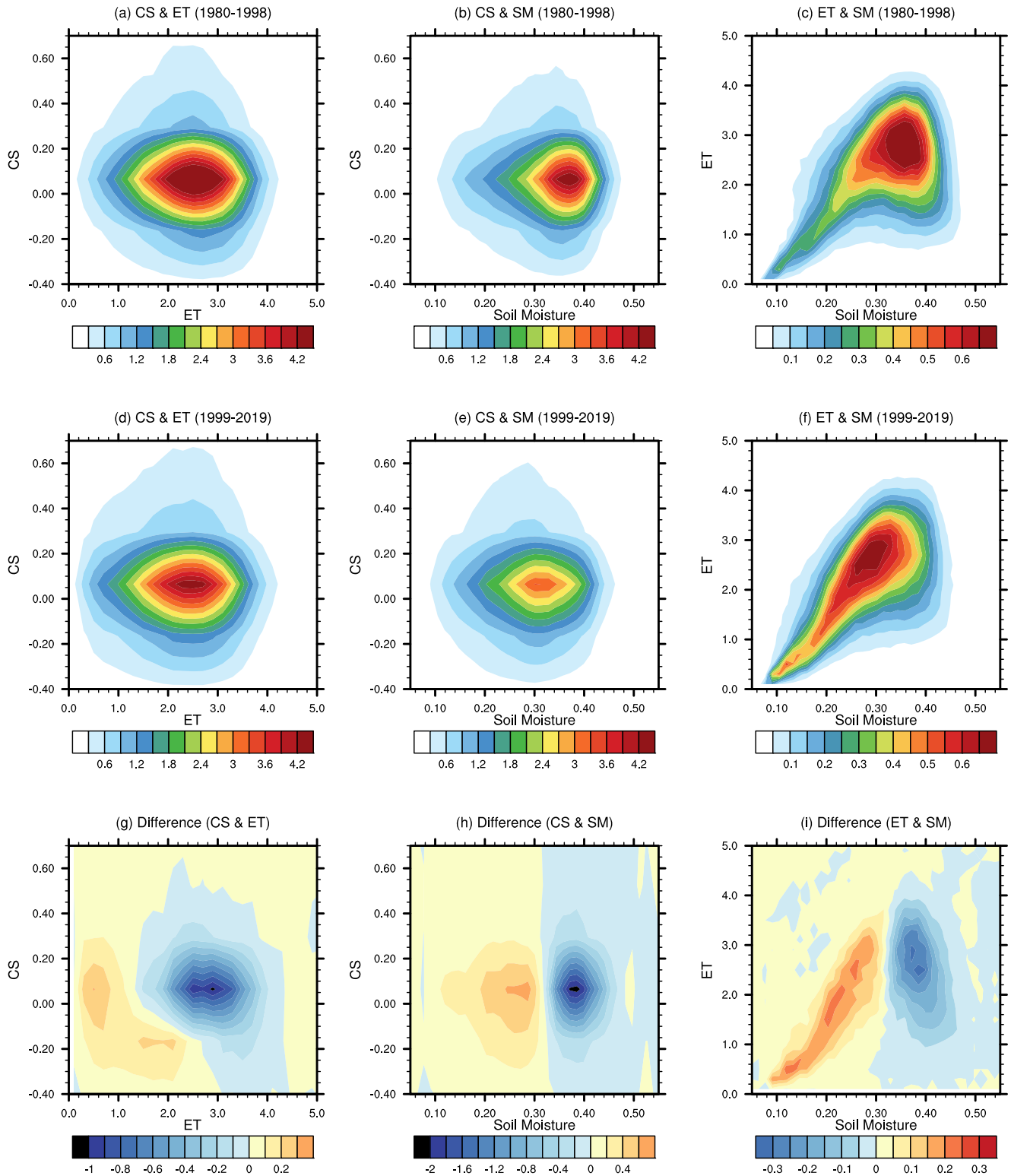


**Fig. 3 Joint probability density function of CS, ET, and SM in summer.** Joint probability density function of (a) soil moisture-temperature coupling strength index (CS) and evapotranspiration (ET) ( $\text{mm day}^{-1}$ ), (b) CS and soil moisture (SM) ( $\text{m}^3 \text{m}^{-3}$ ), and (c) ET and SM in summer (JJA) during (a) 1980–1998 over  $[105\text{--}130^\circ\text{E}, 45\text{--}55^\circ\text{N}]$ . **d–f** Same as (a–c) but for 1999–2019. The differences between two period (1999–2019 and 1980–1998) of joint probability density function of (g) CS and ET, (h) CS and SM, and (i) ET and SM.

strengthens the land–atmosphere interaction over northern East Asia.

To examine the role of persistent soil moisture deficiency on the DHW occurrence, a composite analysis was performed. We selected seven years of persistent soil moisture deficient from

spring to summer (2002, 2006, 2007, 2008, 2011, 2016, and 2017) and five years of only summer soil deficiency (2001, 2004, 2005, 2010, and 2015), based on the standardized soil moisture over the region ( $105^\circ\text{--}130^\circ\text{E}, 45^\circ\text{--}55^\circ\text{N}$ ; Fig. 5). In persistent soil moisture deficient years, more frequent DHW occurred over northern East

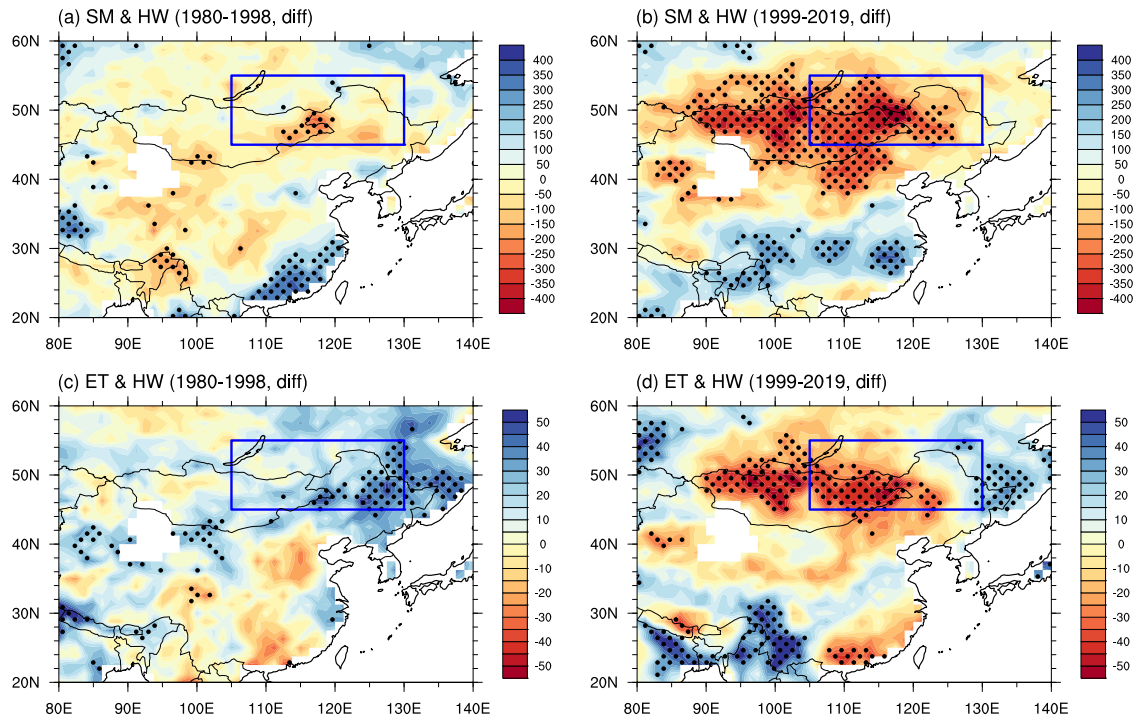


**Fig. 4 Regression of heatwave frequency against seasonal differences of SM and ET.** Regression of heatwave frequency against the seasonal differences of (a, b) soil moisture and (c, d) evapotranspiration between summer (JJA) and spring (MAM) during (a, c) 1980–1998 and (b, d) 1999–2019. The dots denote the 95% confidence level based on the  $P$  values.

Asia, particularly in the regions where the relationship between soil moisture and evapotranspiration changed (Fig. 5c). Heatwaves, which were not considered dry, did not show any significant differences (not shown). This shows that the persistent soil moisture deficiency from spring strengthens of land–atmosphere interaction over northern East Asia. Therefore, changes in the relationship between evapotranspiration and soil moisture due to a lack of soil moisture have amplified the interaction between the surface and the atmosphere and intensified dry heatwave events since the late 1990s.

## DISCUSSION

This study examined the changes in land–atmosphere interaction affecting increases in compound extreme event occurrences over northern East Asia. In particular, we focused on the seasonal changes in soil moisture and evapotranspiration between summer and spring. The distinctive characteristic of soil moisture and atmosphere feedback is soil moisture persistence called soil moisture memory<sup>43</sup>. The role of soil moisture is similar to that of slowly changing components in triggering climate persistence, such as ice, snow, or sea surface temperature<sup>17</sup>. Thus, soil moisture can be a valid precursor in climate prediction because it has relatively gradual variations, from several weeks to several months, and sometimes several seasons<sup>33</sup>. In a further study, the sub-seasonal approach in terms of soil moisture memory can contribute to improving the predictions of extreme summer temperature events.

The enhancement of land–atmosphere interactions induced by soil moisture deficiency over the past two decades, from 1999 to 2019 has been investigated. It is clear that soil moisture declined over northern East Asia after the late 1990s; however, the reasons for the soil drought have not yet been elucidated. We do not doubt that global warming is the primary factor; however, it is necessary to distinguish the effects of anthropogenic forcing and natural variability in decreasing soil moisture over northern East

Asia. These studies may provide a more informative and dependable basis for the changes in compound extreme heat events and need to be further explored in future work.

Human activities such as fertilization, cropping, and irrigation also directly influence vegetation–soil moisture interaction. Changes in land use by humans can strongly affect the seasonal relationships between vegetation and soil moisture<sup>44</sup>. For instance, in China, soil moisture deficiency has increased as agricultural production has increased in recent decades<sup>45</sup>. Understanding the relationship between soil moisture and vegetation can help in understanding land surface development processes and biogeochemical balances, especially in dry regions.

## METHODS

### Definition of compound droughts and heatwaves (DHW)

A heatwave event was defined as temperatures exceeding the 90th percentile of the daily mean temperature during the extended summer season of the Northern Hemisphere (May to October) for at least three consecutive days<sup>46–48</sup>. We selected the summer season, which is highly affected by such heat events. Moreover, considering the low latitude regions where summer starts relatively early, the extended summer was chosen instead of June–July–August (JJA). The 90th percentile was calculated as a single threshold for the total period from 1980 to 2019. To characterize the heatwaves, the total duration (days year<sup>−1</sup>) of the heatwaves that caused human suffering and unhealthy thermal exposure during the entire warm season was analyzed. The total number of heatwaves represents the sum of the heatwave days per year. Compound droughts and heatwaves (DHW) were defined as heatwaves that co-occurred with severely dry conditions. Severely dry conditions were defined as a scPDSI is below  $-3$ .

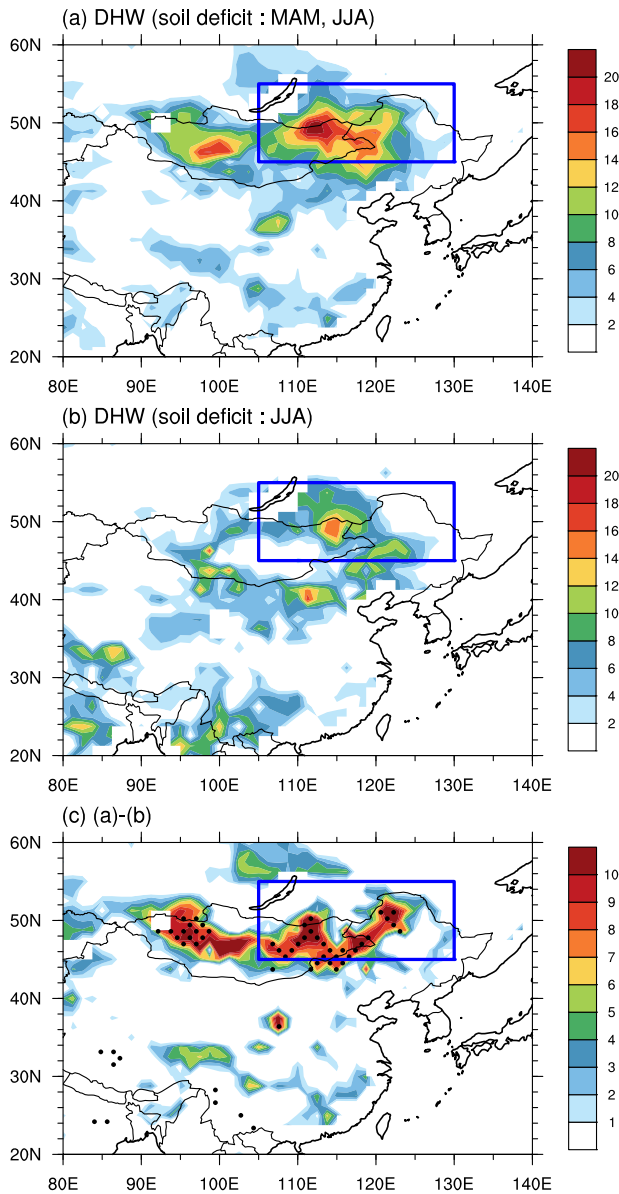


**Fig. 5** Composite map of DHW during soil moisture deficient years. Composite maps of DHW (days year<sup>-1</sup>) for (a) persistent soil moisture deficient years from spring to summer and (b) summer soil moisture deficient years, and (c) difference between (a) and (b). The dots denote the 90% confidence level based on the  $P$  values.

### Soil moisture–temperature coupling matrix

Over East Asia, a diagnostic method to estimate soil moisture–temperature coupling<sup>32</sup> based on two energy balances of evapotranspiration and potential evapotranspiration is used to determine the related heating processes between land and atmosphere. Based on daily data, this method derives the soil moisture–temperature coupling on a daily scale, and the metric ( $\pi$ ) is defined as:

$$\pi = e' \times T' = [H' - H'_p] \times T' = [(R_n - \lambda E) - (R_n - \lambda E_p)] \times T' \quad (1)$$

where  $R_n$  refers to the surface net radiation,  $T'$  represents the anomalies of  $T$ ,  $E$  and  $E_p$  denote the actual and potential evaporation, respectively, and  $\lambda$  is the latent heat of vaporization. The  $e'$  is represented by  $H' - H'_p$  and denotes the contribution of soil moisture deficiency to sensible heat flux. These anomalies are

related to seasonal expectations. The climatological expectation was calculated for each day of the year as the average of the entire multi-year (1980–2019) dataset for that particular day of the year, and then a 31-day moving average was applied.

The energy term  $e'$  will be zero when the soil moisture is sufficient for the atmospheric demand, and it may increase under dry conditions. The positive values of  $\pi$  mean the stronger soil moisture–temperature coupling. The local energy balance only controls the atmospheric temperature if the potential effect of soil moisture on temperature is accompanied by large anomalous temperature values<sup>19</sup>.

### Identification of study area

To further investigate the possible associations between DHW and land–atmosphere interaction, 105°–130°E, and 45°–55°N have been selected as target regions for the DHW. This region is located in the middle-high latitudes and spans northeastern China and eastern Mongolia, features arid and semi-arid climates. The study area exhibits a strong positive linear trend in both DHW and soil moisture–temperature coupling strength (Fig. 1b, d). It is one of the hotspots of regime change in land–atmosphere interaction<sup>3,4,10</sup>.

### Change point detection

To identify significant change points of DHW over the region [105°–130°E, 45°–55°N], we used the Pettitt test<sup>49</sup>. The Pettitt test, a non-parametric statistical test, is commonly used to detect a single change point with continuous data and is useful for examining the remarkable changes in climatic records. Given the time series, the change point of the time series exists at  $K_t$ ,

$$K_t = \max |U_{t,T}| \quad (2)$$

where

$$U_{t,T} = \sum_{i=1}^t \sum_{j=t+1}^T \text{sgn}(X_i - X_j), 1 \leq t < T \quad (3)$$

Pettitt defines the approximate  $p$  value of the test as follows:

$$p \approx 2 \exp\left(\frac{-6K_t^2}{T^3 + T^2}\right) \quad (4)$$

If the  $p$  value is lower than the given significance level, a significant change point exists, and the time series can be divided into two parts at the change point's location.

Before change point detection, the interannual variation in DHW was removed through the 7-year running mean (Supplementary Fig. 1). The year 1999 was detected as a change point for DHW at the 90% confidence level.

### Composite analysis

To further investigate the differences in land–atmosphere coupling strength (CS) according to soil moisture amount, the composite analysis is performed. The wet and dry soil years are defined, if the standardized summer soil moisture over the region [105°–130°E, 45°–55°N] are  $> +1$  and  $< -1$ , respectively. We selected seven wet soil years (1983, 1984, 1985, 1988, 1990, 1993, and 1998) and eight dry soil years (2001, 2002, 2004, 2007, 2008, 2015, 2016, and 2017). Significance levels for the composite analyses are examined by Student's  $t$  test.

### Data

The datasets analyzed in this study are 2 m daily air temperature and upward and downward shortwave radiation fluxes at the surface from JRA-55<sup>50</sup>. For validation and analysis, ERA-Interim data from the European Center for Medium-Range Weather Forecasts was used<sup>51</sup>. Monthly self-calibrating Palmer Drought

Severity Index (scPDSI)<sup>52</sup> data were obtained from Climate Research Unit v4.05 to detect drought events. The scPDSI automatically calibrates the behavior of the PDSI and is used to detect relative dryness. This is the basis of the concept of supply and demand in the water balance equation, thus integrating pre-precipitation, runoff, moisture supply, and evaporation demand at the surface level. A previous study validated that the spatial comparability of the scPDSI was better than that of the PDSI in China<sup>53</sup>, therefore, the scPDSI was used in this study. The scPDSI data for the global land surface (excluding Antarctica) provided a spatial resolution of  $0.5^\circ \times 0.5^\circ$  and a monthly temporal resolution. The Global Land Evapotranspiration model from Amsterdam (GLEAM) v3.5a data<sup>54</sup> was used to examine the soil moisture and temperature coupling metrics. The GLEAM datasets were used to estimate the daily actual evaporation, potential evaporation, evapotranspiration, and surface soil moisture from 1980 to 2019 using satellite data with a  $0.25^\circ \times 0.25^\circ$  spatial resolution.

## DATA AVAILABILITY

JRA-55 reanalysis dataset were accessed from [https://jra.kishou.go.jp/JRA-55/index\\_en.html](https://jra.kishou.go.jp/JRA-55/index_en.html). ERA-Interim reanalysis dataset are used from <https://apps.ecmwf.int/datasets/data/interim-full-daily/>. The scPDSI data are available through <https://crudata.uea.ac.uk/cru/data/drought/>. The GLEAM data can be obtained via <https://www.gleam.eu/>.

## CODE AVAILABILITY

The NCL codes used to run the analysis can be obtained upon request to the corresponding authors.

Received: 13 June 2022; Accepted: 1 December 2022;  
Published online: 15 December 2022

## REFERENCES

- Zscheischler, J. & Seneviratne, S. I. Dependence of drivers affects risks associated with compound events. *Sci. Adv.* **3**, 1–11 (2017).
- Li, X. et al. Concurrent droughts and hot extremes in northwest China from 1961 to 2017. *Int. J. Climatol.* **39**, 2186–2196 (2019).
- Kong, Q., Guerreiro, S. B., Blenkinsop, S., Li, X. F. & Fowler, H. J. Increases in summertime concurrent drought and heatwave in Eastern China. *Weather Clim. Extrem.* **28**, 100242 (2020).
- Yu, R. & Zhai, P. More frequent and widespread persistent compound drought and heat event observed in China. *Sci. Rep.* **10**, 1–7 (2020).
- Wang, J. et al. Anthropogenically-driven increases in the risks of summertime compound hot extremes. *Nat. Commun.* **11**, 528 (2020).
- Rippey, B. R. The U.S. drought of 2012. *Weather Clim. Extrem.* **10**, 57–64 (2015).
- Ruffault, J. et al. Increased likelihood of heat-induced large wildfires in the Mediterranean Basin. *Sci. Rep.* **10**, 1–9 (2020).
- Filipa Silva Ribeiro, A., Russo, A., Gouveia, C. M., Páscoa, P. & Zscheischler, J. Risk of crop failure due to compound dry and hot extremes estimated with nested copulas. *Biogeosciences* **17**, 4815–4830 (2020).
- Mazdiyasi, O. & AghaKouchak, A. Substantial increase in concurrent droughts and heatwaves in the United States. *Proc. Natl Acad. Sci.* **112**, 11484–11489 (2015).
- Zhang, P. et al. Abrupt shift to hotter and drier climate over inner East Asia beyond the tipping point. *Science* **370**, 1095–1099 (2020).
- Almazroui, M. et al. Projected changes in climate extremes using CMIP6 simulations over SREX regions. *Earth Syst. Environ.* **5**, 481–497 (2021).
- Zhou, S. et al. Land-atmosphere feedbacks exacerbate concurrent soil drought and atmospheric aridity. *Proc. Natl Acad. Sci. USA* **116**, 18848–18853 (2019).
- Kumar, S. et al. Terrestrial contribution to the heterogeneity in hydrological changes under global warming. *Water Resour. Assoc.* **52**, 3127–3142 (2016).
- Mukherjee, S. & Mishra, A. K. Increase in compound drought and heatwaves in a warming world. *Geophys. Res. Lett.* **48**, 1–13 (2021).
- Seo, Y.-W., Ha, K.-J. & Park, T.-W. Feedback attribution to dry heatwaves over East Asia. *Environ. Res. Lett.* **16**, 064003 (2021).
- Seneviratne, S. I., Lüthi, D., Litschi, M. & Schär, C. Land-atmosphere coupling and climate change in Europe. *Nature* **443**, 205–209 (2006).
- Lorenz, R., Jaeger, E. B. & Seneviratne, S. I. Persistence of heat waves and its link to soil moisture memory. *Geophys. Res. Lett.* **37**, 1–5 (2010).
- Alexander, L. Climate science: Extreme heat rooted in dry soils. *Nat. Geosci.* **4**, 12–13 (2011).
- Miralles, D. G., Teuling, A. J., Van Heerwaarden, C. C., & De Arellano, J. V. G. Mega-heatwave temperatures due to combined soil desiccation and atmospheric heat accumulation. *Nat. Geosci.* **7**, 345–349 (2014).
- Miralles, D. G., Gentile, P., Seneviratne, S. I. & Teuling, A. J. Land-atmospheric feedbacks during droughts and heatwaves: state of the science and current challenges. *Ann. NY Acad. Sci.* **1436**, 19–35 (2019).
- Fischer, E. M., Seneviratne, S. I., Vidale, P. L., Luthi, D. & Schar, C. Soil moisture-atmosphere interactions during the 2003 European Summer Heat Wave. *J. Clim.* **20**, 5081–5099 (2007).
- Koster, R. D. et al. GLACE: the global land-atmosphere coupling experiment. Part I: Overview. *J. Hydrometeorol.* **7**, 590–610 (2006).
- Whan, K. et al. Impact of soil moisture on extreme maximum temperatures in Europe. *Weather Clim. Extrem.* **9**, 57–67 (2015).
- Perkins, S. E., Argüeso, D. & White, C. J. Relationships between climate variability, soil moisture, and Australian heatwaves. *J. Geophys. Res. Atmos.* **120**, 8144–8164 (2015).
- Wang, P., Zhang, Q., Yang, Y. & Tang, J. The sensitivity to initial soil moisture for three severe cases of heat waves over eastern China. *Front. Environ. Sci.* **7**, 1–16 (2019).
- Li, K., Zhang, J., Yang, K. & Wu, L. The role of soil moisture feedbacks in future summer temperature change over East Asia. *J. Geophys. Res. Atmos.* **124**, 12034–12056 (2019).
- Berg, A. et al. Land-atmosphere feedbacks amplify aridity increase over land under global warming. *Nat. Clim. Chang.* **6**, 869–874 (2016).
- Vogel, M. M. et al. Regional amplification of projected changes in extreme temperatures strongly controlled by soil moisture-temperature feedbacks. *Geophys. Res. Lett.* **44**, 1511–1519 (2017).
- Zampieri, M. et al. Hot European summers and the role of soil moisture in the propagation of mediterranean drought. *J. Clim.* **22**, 4747–4758 (2009).
- Rohini, P., Rajeevan, M. & Srivastava, A. K. On the variability and increasing trends of heat waves over India. *Sci. Rep.* **6**, 1–9 (2016).
- Ha, K.-J. et al. Dynamics and characteristics of dry and moist heatwaves over East Asia. *npj Clim. Atmos. Sci.* **5**, 1–11 (2022).
- Miralles, D. G., van den Berg, M. J., Teuling, A. J. & de Jeu, R. A. M. Soil moisture-temperature coupling: A multiscale observational analysis. *Geophys. Res. Lett.* **39**, L21707 (2012).
- Dirmeyer, P. A., Schlosser, C. A. & Brubaker, K. L. Precipitation, recycling, and land memory: An integrated analysis. *J. Hydrometeorol.* **10**, 278–288 (2009).
- Gao, C., Li, G., Chen, H. & Yan, H. Interdecadal change in the effect of spring soil moisture over the indo-China peninsula on the following summer precipitation over the yangtze river Basin. *J. Clim.* **33**, 7063–7082 (2020).
- Seneviratne, S. I. et al. Investigating soil moisture-climate interactions in a changing climate: A review. *Earth-Sci. Rev.* **99**, 125–161 (2010).
- Sato, T. & Xue, Y. Validating a regional climate model's downscaling ability for East Asian summer monsoonal interannual variability. *Clim. Dyn.* **41**, 2411–2426 (2013).
- Erdenebat, E. & Sato, T. Role of soil moisture-atmosphere feedback during high temperature events in 2002 over Northeast Eurasia. *Prog. Earth Planet. Sci.* **5**, 37 (2018).
- Zaitchik, B. F., Macalady, A. K., Bonneau, L. R. & Smith, R. B. Europe's 2003 heat wave: A satellite view of impacts and land - Atmosphere feedbacks. *Int. J. Climatol.* **26**, 743–769 (2006).
- Seneviratne, S. I., Donat, M. G., Mueller, B. & Alexander, L. V. No pause in the increase of hot temperature extremes. *Nat. Clim. Chang.* **4**, 161–163 (2014).
- Yuan, Q. et al. Coupling of soil moisture and air temperature from multiyear data during 1980–2013 over china. *Atmosphere* **11**, 25 (2020).
- Koster, R. D., Schubert, S. D. & Suarez, M. J. Analyzing the concurrence of meteorological droughts and warm periods, with implications for the determination of evaporative regime. *J. Clim.* **22**, 3331–3341 (2009).
- Hirschi, M.-C. et al. Soil moisture and evapotranspiration. Hydro- CH2018 project. (2020) <https://doi.org/10.3929/ethz-b-000389455>.
- Koster, R. D. & Suarez, M. J. Soil moisture memory in climate models. *J. Hydrometeorol.* **2**, 558–570 (2001).
- Lian, X. et al. Summer soil drying exacerbated by earlier spring greening of northern vegetation. *Sci. Adv.* **6**, 1–12 (2020).
- Wang, S., Fu, B. J., Gao, G. Y., Yao, X. L. & Zhou, J. Soil moisture and evapotranspiration of different land cover types in the Loess Plateau, China. *Hydrol. Earth Syst. Sci.* **16**, 2883–2892 (2012).
- Meehl, G. A. & Tebaldi, C. More intense, more frequent, and longer lasting heat waves in the 21st century. *Science* **305**, 994–997 (2004).
- Perkins, S. E. & Alexander, L. V. On the measurement of heat waves. *J. Clim.* **26**, 4500–4517 (2013).
- Russo, S. et al. Magnitude of extreme heat waves in present climate and their projection in a warming world. *J. Geophys. Res. Atmos.* **119**, 12500–12512 (2014).
- Pettit, A. N. A non-parametric approach to the change-point problem. *J. R. Stat. Soc. Ser. C (Appl. Stat.)* **28**, 126–135 (1979).

50. Kobayashi, C. & Iwasaki, T. Brewer-Dobson circulation diagnosed from JRA-55. *J. Geophys. Res. Atmos.* **121**, 1493–1510 (2016).
51. Dee, D. P. et al. The ERA-Interim reanalysis: Configuration and performance of the data assimilation system. *Q. J. R. Meteorol. Soc.* **137**, 553–597 (2011).
52. van der Schrier, G., Barichivich, J., Briffa, K. R. & Jones, P. D. A scPDSI-based global data set of dry and wet spells for 1901–2009. *J. Geophys. Res. Atmos.* **118**, 4025–4048 (2013).
53. Zhong, Z., He, B. I. N., Guo, L. & Zhang, Y. Performance of various forms of the palmer drought severity index in China from 1961 to 2013. *J. Hydrometeorol.* **20**, 1867–1885 (2019).
54. Martens, B. et al. GLEAM v3: Satellite-based land evaporation and root-zone soil moisture. *Geosci. Model Dev.* **10**, 1903–1925 (2017).

## ACKNOWLEDGEMENTS

This study was supported by the Institute for Basic Science (project code IBS-R028-D1).

## AUTHOR CONTRIBUTIONS

K.-J.H. and Y.-W.S. designed and conceived the research, Y.-W.S. contributed to the graphics and analyzed, K.-J.H. and Y.-W.S. wrote the early draft and contributed to writing the manuscript.

## COMPETING INTERESTS

The authors declare no competing interests.

## ADDITIONAL INFORMATION

**Supplementary information** The online version contains supplementary material available at <https://doi.org/10.1038/s41612-022-00325-8>.

**Correspondence** and requests for materials should be addressed to Kyung-Ja Ha.

**Reprints and permission information** is available at <http://www.nature.com/reprints>

**Publisher's note** Springer Nature remains neutral with regard to jurisdictional claims in published maps and institutional affiliations.



**Open Access** This article is licensed under a Creative Commons Attribution 4.0 International License, which permits use, sharing, adaptation, distribution and reproduction in any medium or format, as long as you give appropriate credit to the original author(s) and the source, provide a link to the Creative Commons license, and indicate if changes were made. The images or other third party material in this article are included in the article's Creative Commons license, unless indicated otherwise in a credit line to the material. If material is not included in the article's Creative Commons license and your intended use is not permitted by statutory regulation or exceeds the permitted use, you will need to obtain permission directly from the copyright holder. To view a copy of this license, visit <http://creativecommons.org/licenses/by/4.0/>.

© The Author(s) 2022